ELSEVIER

Behavioural Brain Research 84 (1997) 117–127

BEHAVIOURAL BRAIN RESEARCH

Research report

Modulation of inhibition in a model of olfactory bulb reduces overlap in the neural representation of olfactory stimuli

Christiane Linster *, Michael Hasselmo

Department of Psychology and Program in Neuroscience, Harvard University, 33, Kirkland Street (Room 1446), Cambridge, MA 02138, USA

Received 28 February 1996; revised 21 June 1996; accepted 21 June 1996

Abstract

In a neural model of olfactory bulb processing, we demonstrate the putative role of the modulation of two types of inhibition, inspired by electrophysiological data on the effect of acetylcholine and noradrenaline on olfactory bulb synaptic transmission. Feedback regulation of modulation based on bulbar activity serves to 'normalize' the activity of output neurons in response to different levels of input activities. This mechanism also decreases the overlap between pairs of output patterns (Mitral cell activities), enhancing the discrimination between overlapping olfactory input patterns. The effect of the modulation at the two levels of interneurons is complementary: while an increase in periglomerular inhibition decreases the number of responding output neurons, a decrease in granule cell inhibition increases the firing frequencies of these neurons.

Keywords: Olfactory bulb; Feedback; Modulation of inhibition; Neuromodulation; Computer model

1. Introduction

The olfactory bulb is the first relay structure of olfactory processing in vertebrates. The information received from the olfactory epithelium is conveyed to higher brain structures, more particularly the olfactory (piriform) cortex, by two categories of relay neurons: mitral and tufted cells. Most experimental data suggest that the olfactory bulb (OB) plays a critical role in feature extraction, noise reduction and contrast enhancement (for reviews see [16,38]), whereas more cognitive functions such as the associative storage of olfactory information would be located in the olfactory cortex [10]. Olfactory bulb processing relies on interactions of mitral/tufted cells with two main classes of local interneurons: periglomerular cells and granule cells which mediate inhibition at two levels of processing in the olfactory bulb: periglomerular cells cause inhibitory potentials on the mitral cell primary dendrites in the outer glomerular layer, whereas granule cells induce inhibitory potentials on mitral cell secondary dendrites in the deeper external plexiform layer. The olfactory bulb neurons integrate information not only from intrabulbar neurons, but also from numerous centrifugal structures, including piriform cortex, telencephalic basal forebrain and the brain stem locus coerulus. More particularly, a noradrenergic (NA) input from the locus coerulus (LC) synapses mainly in the mitral cell and granule cell layers, whereas cholinergic (ACh) input from the horizontal limb of the diagonal band of Brocca (HDB) innervates all layers of the olfactory bulb, but mainly the glomerular layer (for review see [11,28]). Behavioral investigations on the role of centrifugal input have shown that noradrenergic bulbar modulation is critical for long term storage of information in mice in the accessory olfactory bulb [1], in the main olfactory bulb in sheep [21,32] and in new born rats [39]. Bulbar cholinergic modulation could be associated with short-term olfactory memory [35].

NA modulation has been shown to suppress inhibition of mitral cells by granule cells, at least partly through suppression of the excitation of granule cells by mitral cells [16,35]; ACh has been shown to suppress inhibition of mitral cells by granule cells [5] while it appears to increase periglomerular cell firing [31] when applied to

* Corresponding author. Tel.: (617) 495 3875; Fax: (617) 495 3728; E-mail: linster@katla.harvard.edu

PII S0166-4328(96)00141-6

the glomerular layer. Here, we will show how the modulation of inhibition at the two levels of interneurons could contribute to the filtering and feature extraction role of the olfactory bulb.

Recent models of piriform cortex processing have demonstrated that this structure could mediate associative storage of olfactory information [13,14]. Experimental and modeling data have shown the importance of ACh modulation for the regulation of cortical dynamics between storage of new information and recall of previously experienced information [15]. The problem of deciding between recall and storage states can be solved by a feedback regulation mechanism based on cortical activity [12,15]. In a recently developed neural model of the olfactory bulb [25,26], we have analyzed the putative role of the two layers of inhibition for information processing in the olfactory bulb. In this paper, we extend these results. We show how regulation of the modulation of both types of inhibition by mitral cell activity can serve to 'normalize' olfactory input and to reduce the overlap between patterns of activity.

2. Methods

A more extensive description of the model architecture has been given elsewhere [25] and the equations we used for neurons and synaptic transmission are those presented before [27]. A detailed description of the relevant parameters is given in Appendix A

The model includes four categories of neurons (Fig. 1): receptor cells, mitral cells, periglomerular cells and granule cells. All categories of neurons are represented as single-compartments, except for mitral cells, for which primary and secondary dendrites are represented as separate compartments. Each neuron is characterized by its specific time constant, which can be regarded as the mean product of the membrane resistance and capacitance. The output of the neurons are discrete spikes, computed according to the instantaneous spiking probability (which is a continuous, bounded function of the membrane potential).

In the model, 15 types of receptor cells with overlapping molecular response properties are represented which can be differentially activated by 15 different odorant components. The receptor cells project onto 15 glomeruli; each of these glomeruli represents a glomerular population receiving converging input from one type of receptor cell. Receptor cells synapse onto primary dendrites of mitral cells as well as onto periglomerular cell dendrites (Fig. 1). Mitral cell primary dendrites excite periglomerular cells which in turn inhibit mitral cells. Periglomerular cells send lateral connections onto neighboring glomeruli (these lateral interactions span a radius of 2 neighboring glomeruli) where they inhibit mitral cell primary dendrites. The available electrophysiological data shows that periglomerular cells generate action potentials in response to odorant stimuli [44].

Mitral cell primary dendrites integrate all sources of excitation and inhibition transmitted to them inside their glomerulus and transmit this continuous value to their site of integration (cell body) where signals on secondary dendrites undergo spatial and temporal summation and where action potentials can be triggered.

Mitral cell secondary dendrites locally interact with granule cells; each mitral cell interacts, via granule cells, with the secondary dendrites of mitral cells connected to ten neighboring glomeruli. The degree to which one mitral cell produces lateral inhibition in another by way of granule cell activation depends on the mitral cells activity, on the number of common granule cells that both cells contact and on the decline of mitral cell activity along the secondary dendrites. The decline of strength of connections to granule cells at different points along the mitral cell secondary dendrites approximately takes into account the cumulative inhibitory influences of numerous granule cell contacts to these dendrites. Granule cells can locally interact with each other through inhibitory connections [43].

2.1. Modulatory neuron

Feedback regulation of modulation necessitates a modulator neuron (mo) with a relatively long time constant (50 ms) as compared to other time constants in the model, and a higher activation threshold. The modulator neuron receives input from all mitral cells, and computes its output according to: $\mathrm{mo}(t) = f[v(t)]$ where $\mathrm{mo}(t)$ is the modulator neuron output and $v(t)$ its membrane potential.

The membrane potential is described by:

$$\tau \frac{\mathrm{d}v(t)}{\mathrm{d}t} + v(t) = \Sigma \mathrm{mi}(t)$$

where τ is the time constant and $\mathrm{mi}(t)$ are the mitral cell outputs.

f is a linear threshold function with:

$f(x) = 0$ for $x < \theta_{\min}$;

$f(x) = (x - \theta_{\min})/(\theta_{\max} - \theta_{\min})$ for $\theta_{\min} < x < \theta_{\max}$

and

$f(x) = 1$ for $x > \theta_{\max}$ where $\theta_{\min}$, $\theta_{\max}$ are the activation and saturation thresholds.

The modulator neuron feeds back directly onto periglomerular cells with a connection weight which is the variable parameter M_{pg}. Its output activity also modulates the inhibitory connection strength (w^{gm}) between

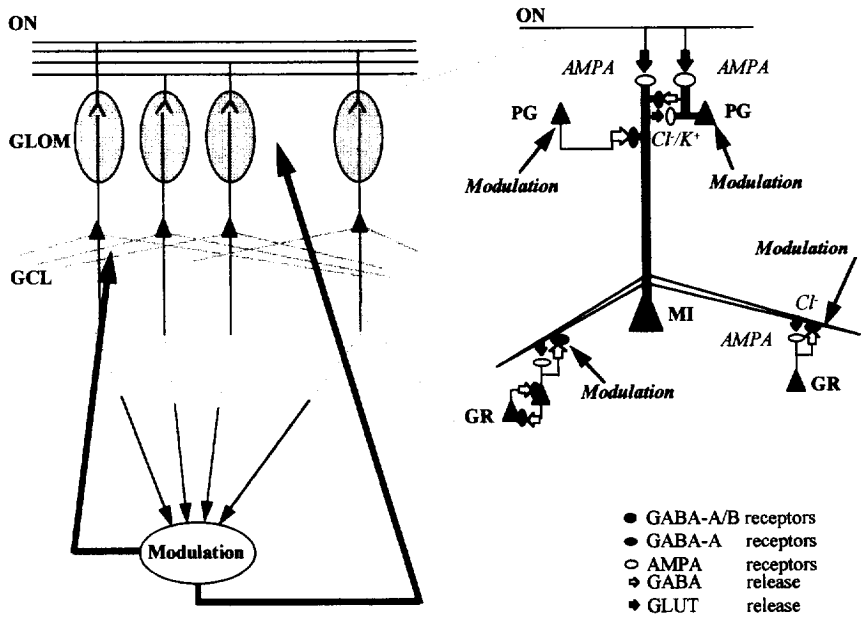

Fig. 1. Schematic representation of the model architecture and the connections. 15 Receptor cells have broad, overlapping sensitivities to 15 odorant components (normalized gaussian function with standard deviation 2). Each receptor cell (ON) projects into one of the 15 glomeruli (GLOM), where it synapses with mitral cell primary dendrites (Mi1_) and periglomerular cells. Reciprocal interactions exist between Mi1_ and periglomerular cells in the glomeruli, in addition, periglomerular cells send inhibitory connections into 5 neighboring glomeruli (to mitral cells and periglomerular cells). The signal resulting from glomerular interactions are conveyed to mitral cell bodies and secondary dendrites (Mi2_) in the deeper layer, where Mi2_ interact with numerous granule cells at long distances through reciprocal connections, the strength of the interactions decays with distance and the transmission delays increase with distance. Neighboring granule cells also interact with each other through a reciprocal feedback connection. The amplitude of the modulatory signal (Modulation) fed back to the OB is a function of the sum of all mitral cell output activity. The modulation acts directly on PG cells and on the connection strengths between mitral cells and granule cells. All parameter values are chosen randomly in a uniform distribution (+/10%) around the given mean values.

granule cells and mitral cells:

$$w^{gm}(t)=(1.0-M_{gm})\mathrm{mo(t)}w^{gm}(\max)$$

where M_{gm} is the variable modulation parameter.

2.2. Input and output space

In the following, we consider a 15 dimensional input space of odorant components. Each stimulus represents a point in this space. Odor stimuli are classified according to the percentages of active components that they comprise. The output space comprises the average instantaneous spiking probabilities of mitral cells connected to each of the 15 glomeruli. These spiking probabilities are classified into 3 types: non-response, suppression or activation. The baseline activity is the average of all mitral cell activity during 2 s of simulation time in the absence of input stimulus. Responses to stimuli are then classified with respect to this average baseline: mitral cell activities are averaged over the duration of the input stimulus (one sniff cycle usually lasts 120 ms), and all values are normalized between -1 and $+1$. A neuron with activity >0.15 is considered active, and a neuron with activity <-0.15 is considered suppressed.

3. Results

The model described here is inspired by and reproduces many of the features previously described in neural models of the olfactory bulb implementing various levels of detail [4,6,23,24,29,33,45]; the parameters have been adjusted until a single parameter set was found which could match single cell data as well as population dynamics described in the literature. The model generates spiking frequencies in the range of those observed experimentally (Fig. 2A and B) [2,3,31,43], as well as responses to simulated olfactory electrical stimulation close to those described by Wellis and Scott [43] (Fig. 2C and D). On the level of population responses, the model simulates field potential recordings in response to electrical stimulation of the olfactory nerve and the lateral olfactory tract (Fig. 2D and E) [5,33] and EEG recordings in response to odor stimulation [8].

3.1. Odor processing

Due to the overlapping odorant spectra of the receptor cells, any particular stimulus activates a large population of glomeruli. Periglomerular cells are activated by receptor cell input and by mitral cell input. The lateral

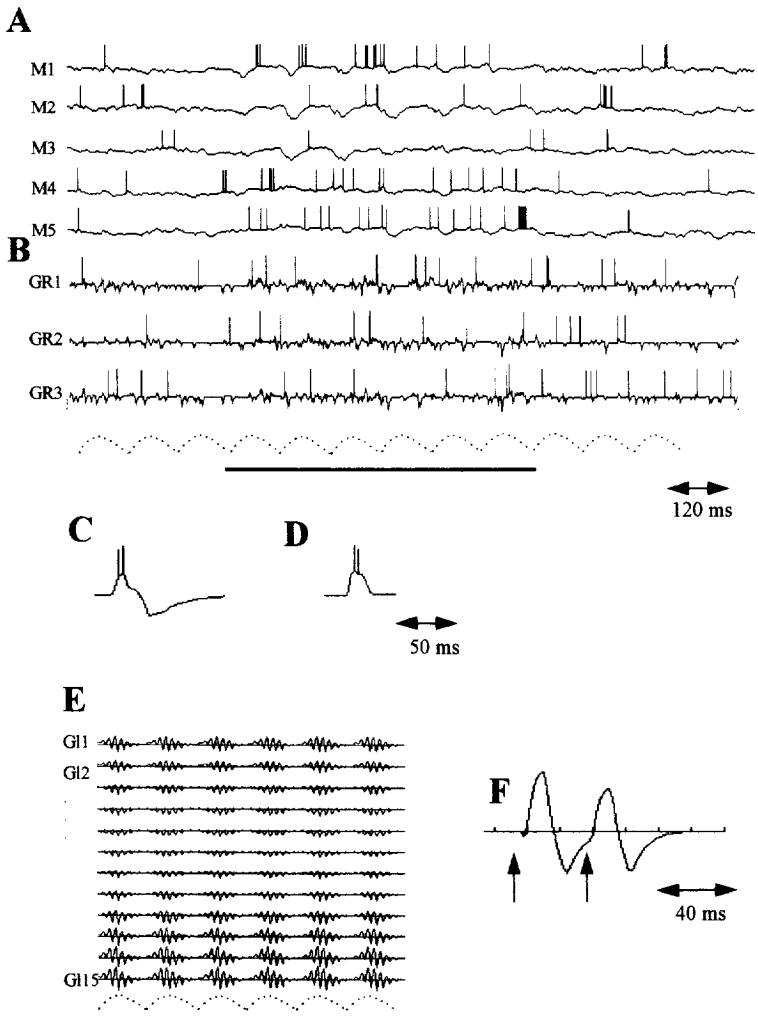

Fig. 2. Individual and population activities in the model in response to odor and electrical stimulation. (A) Membrane potentials and action potentials of Mi cells (M1–M5) in response to odor stimulation. Mi cells respond with changes in their pattern of discharge to stimulation. Mi cell spiking frequencies range from 2 spikes/s in absence of stimulation to 24 spikes/s in the presence of stimulation. This is in the range of observed spiking activities in response to odors in awake rabbits [2,3] and rats [28]. The dotted lines represent a low amplitude, noise input mimicking respiration to which olfactory input (solid line) is added. Stimuli rise towards maximal amplitude during 60 ms, stay at maximal amplitude during 20 ms and fall towards zero during 40 ms. (B) Membrane potentials and action potentials of Gr cells (GR1–GR3) in response to odor stimulation (O). Spiking frequencies for individual Gr cells ranged from 0.2 spikes/s in the absence of odor input to 20 spikes/s in response to odor input; this is comparable to Gr cell activities observed in response to odors in the rat [38]. The dotted lines represent a low amplitude, noise input mimicking respiration to which olfactory input (solid line) is added. (C) Electrical stimulation in the olfactory nerve was simulated by a brief (2 ms) input to all afferent synapses. Gr cells in the model respond with a depolarization of the membrane potential, eliciting one or two spikes, followed by a prolonged inhibition to olfactory nerve stimulation (see [38]). (D) Pg cells respond with a large depolarization, during which one or two spikes can occur in response to olfactory nerve stimulation (see [38] for comparison). (E) Odor-induced evoked field potentials (EFP) computed at 15 locations (corresponding to the columns under each glomerulus) of the model. EFP are computed as the average variations of membrane potentials of GR cells (80%) and of Mi cells (20%). A given olfactory stimulus triggers bursts of oscillatory activity across the model, where different spatial locations oscillate with the same average frequency but with different amplitudes. Fast oscillations (around 60 Hz) are riding on a slow (8 Hz) wave corresponding to stimulus frequency (compare to [7]). (F) Electrically-induced EFP in response to a paired-pulse stimulation. Two brief pulses (2 ms) were delivered to the output fibers of the Mi cells in an 40 ms interval. The positive response to the second pulse is significantly diminished (20%) as compared to the response to the first pulse as a consequence of the long lasting hyperpolarization of the Mi cells in response to the first pulse, as has been described in in vivo experiments in rats [5].

inhibition mediated by periglomerular cells triggers a competition between activated glomeruli which suppresses weakly activated mitral cells. Due to the subsequent effects of granule cell inhibition, weak activation of mitral cell dendrites is further suppressed. The resulting across fiber pattern of mitral cell activities connected to 15 different glomeruli in the model is shown in Fig. 3. In response to three different input stimuli (each comprising a single active component), mitral cells can be either activated (with varying temporal patterns of activity) or inhibited, or can maintain its spontaneous activity pattern. As can be expected due to the lateral inhibition

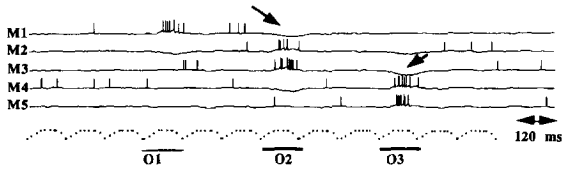

Fig. 3. Activities of 5 mitral cells (M1–M5) connected to 5 of the 15 glomeruli in response to three stimuli (O1–O3) (each comprising a single active component). For each stimulus, a particular mitral cell responds with either an increase, a decrease (arrow) firing frequencies or change in its spontaneous firing. Input stimuli (solid lines) are superimposed on an input noise of low concentration modulated by 8 Hz and mimicking the respiratory input (dashed line).

action among the glomeruli, activated mitral cells are often surrounded by inhibited mitral cells; thus, spots of activation appear. As will be shown below, the radius of the active spots depends on the strength of the lateral inhibition.

A systematic variation of the total amount of lateral inhibition provided by periglomerular cells has shown that there seems to be an optimal range depending on the complexity of the input pattern (we define low complexity input patterns as patterns with few active components, high complexity input patterns as patterns with high percentages of active components). Fig. 4 shows the average percentages of active mitral cells as a function of the total amount of lateral inhibition in the model for three values of input complexity. One can see that if few (10%) odor components are active, only at very low values of lateral inhibition is the total activity strong enough to have active mitral cells emerge. For high input complexity (80% of active components), all mitral cells are activated for all input patterns at low values of lateral inhibition. Thus, for low values of lateral inhibition, no differentiation among input patterns with high complexity is possible at the output.

As a consequence, in order to guarantee optimal information processing, the amount of lateral inhibition should be variable as a function of the amount of activity conveyed by the receptor cells. This is what the feedback regulation via the modulator neuron is supposed to provide. In the following, we first demonstrate (i) the effect of feedback regulation of the modulation of periglomerular cells; (ii) the effect of feedback regulation of the modulation of granule cell inhibition; and (iii) the effect of combined feedback regulation of the modulation of periglomerular cells and of granule cell inhibition.

3.2. Modulation of periglomerular cell activity

The initial parameters are set to low values of lateral inhibition optimal for processing of low complexity input patterns. In addition, the activation threshold of the Mo neuron is set such that it is not activated for low levels of total mitral cell activity in response to low complexity input patterns. If more mitral cells are recruited, the feedback regulation increases periglomerular cell activation and in return decreases the number of active mitral cells. Fig. 5 shows the average percentages of activated mitral cells as a function of input pattern complexity for varying levels of feedback modulation of periglomerular cells (M_{pg}) in the absence of modulation of granule cell inhibition ($M_{gm}=0.0$). At the maximum level ($M_{pg}=3$),

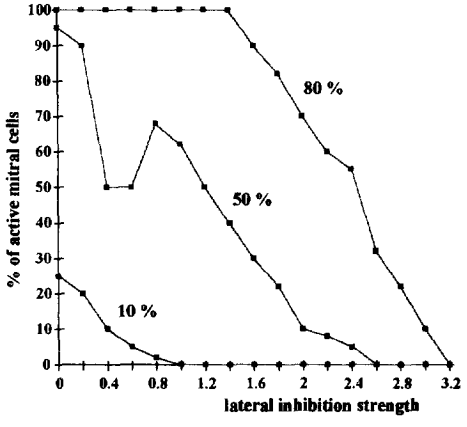

Fig. 4. Percentages of active mitral cells as a function of lateral inhibition strength and input pattern complexity. For each value of input pattern complexity, 100 random input patterns were created and the percentages of active mitral cells in response to these input patterns were averaged (see Section 2: Methods). For each simulation, a different set of parameter values was used, within the distributions described in the appendix. If only a few (10%) odor components are active, the total activity is only strong enough to have active mitral cells emerge at very low values of lateral inhibition. For high input complexity (80% of active components), all mitral cells are activated for all input patterns at low values of lateral inhibition.

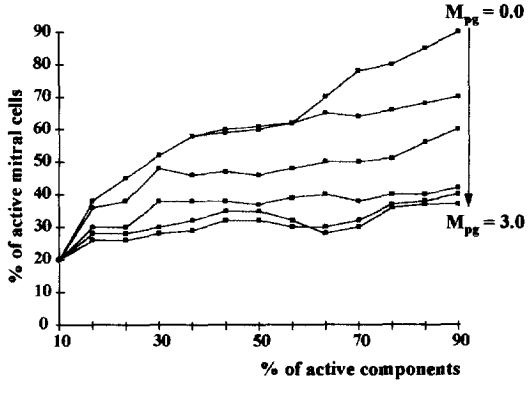

Fig. 5. Percentage of active mitral cells as a function of input pattern complexity for different values of feedback modulation of periglomerular cells. For each value of input pattern complexity, 100 random input patterns were created, and the percentages of active mitral cells in response to these inputs were averaged. Average numbers of non-responsive mitral cells stay relatively constant for all M_{PG} values used (not shown). The curves show the average percentages of activated mitral cells as a function of input pattern complexity for varying levels of feedback modulation of periglomerular cells (M_{pg}) in the absence of modulation of granule cell inhibition ($M_{gm}=0.0$). At the maximum level ($M_{pg}=3$), the number of active mitral cells stays almost constant over input pattern space.

the number of active mitral cells stays almost constant over input pattern space.

3.3. Modulation of granule cell inhibition

The activity pattern conveyed to the deeper cell layers from the glomeruli is regulated by a second, much more broadly distributed, inhibition from the granule cells.

The model shows that for a very large range of granule cell inhibition, the proportion of mitral cells responding to a large set of odorants remains unchanged; however, a decrease of granule cell inhibition almost linearly increases the spiking frequencies of those cells which are activated by the stimulus. Thus, for a given number of activated mitral cells (determined by the processing in the glomerular layer), the amplitude of the mitral cell responses is influenced by the strength of granule cell inhibition. Furthermore, with low levels of inhibition, the response probability to low concentration stimuli can be enhanced.

Fig. 6 shows the effect of regulation of the modulation of granule cell inhibition (in the absence of modulation of periglomerular cell activity) on the firing frequencies of activated mitral cells as a function of input pattern complexity. While the average number of activated mitral cells does not change (for $M_{gm}=0$ as compared to $M_{gm}=0.9$, Fig. 6A), the average firing probabilities of these mitral cells increase considerably for higher input pattern complexity (Fig. 6B).

3.4. Overlap between input and output patterns

Limiting the number of mitral cells responding to complex input patterns is not useful by itself for the filtering function of the olfactory bulb unless it leads to less overlap between pairs of output patterns. Especially for complex input patterns, a separation of these patterns in the output space can be crucial for successful storage and recall in higher brain centers.

In order to address this problem, we have computed the normalized scalar-products between pairs of input patterns and the resulting pairs of output patterns (Fig. 7) for varying levels of M_{pg}. Without feedback modulation, the amount of overlap between output patterns increases almost linearly with the amount of overlap between input patterns ($M_{pg}=0.0$). With increasing modulation however, the overlap between output patterns is significantly lower than the overlap between input patterns. Thus, feedback modulation of lateral inhibition not only normalizes the total amount of activity in the mitral cell output, but also considerably decreases the overlap between pairs of output patterns.

As an illustration, Fig. 8 shows the activity patterns in the network with no feedback modulation ($M_{pg}=0.0$ and $M_{gm}=0.0$) and with maximal feedback modulation ($M_{pg}=3.0$ and $M_{gm}=0.9$) for two pairs of input patterns with low complexity (6%, Fig. 8A) and high complexity

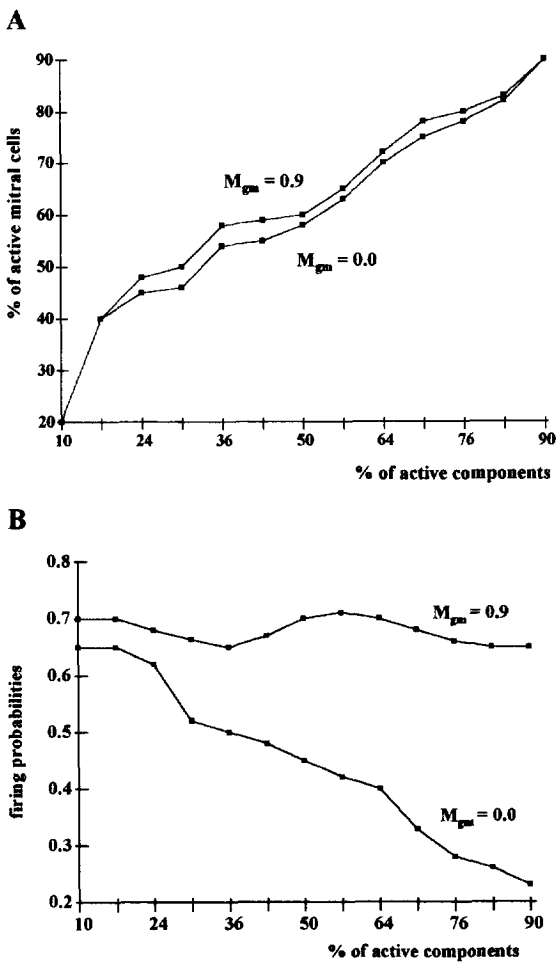

Fig. 6. Effect of modulation of granule cell inhibition on mitral cell activity. (A) Minimal ($M_{gm}=0$) and maximal ($M_{gm}=0.9$) modulation values are shown. The average number of active mitral cells as a function of input complexity is nor influenced by the modulation (M_{gm}). (B) In absence of modulation ($M_{gm}=0$) the average firing probabilities of active mitral cells decreases as a function of input complexity. In contrast, maximal modulation ($M_{gm}=0.9$) leads to constant firing probabilities over input space.

(60%, Fig. 8B). In Fig. 8A, one odorant component is activated in each stimulus. In both cases, due to the broad sensitivity spectra of receptor cells, a population of glomeruli receives input (Glom). A comparison between the figures shows that there is no difference in the activity patterns of periglomerular cells (periglomerular) and mitral cells (mitral) with or without modulation. In contrast, in Fig. 8B, the modulation is activated, and the periglomerular cells exhibit much higher activation levels with modulation than without modulation. This results in more lateral inhibition exerted onto mitral cells, and in a considerable decrease of activated mitral cells. In this example the overlap between the input patterns is 0.63. The overlap between the output patterns is even greater (0.66) without modulation, and considerably decreased with maximum modulation (0.26). The few activated mitral cells exhibit high spiking probabili-

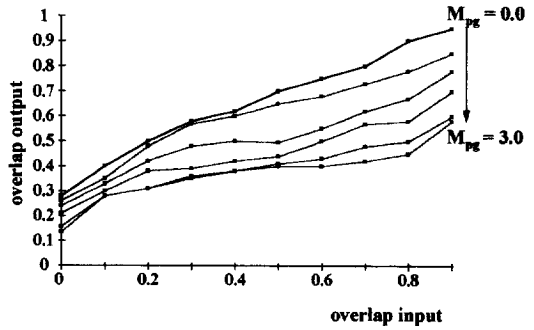

Fig. 7. Overlap of mitral cell activity patterns as a function of input pattern overlap and increasing periglomerular cell modulation M_{pg}. Overlap between pairs of input patterns and between the corresponding output patterns is computed as normalized scalar products (scalar products divided by the number of active components). The curves show the overlap between pairs of output patterns as a function of the overlap between the corresponding input patterns for increasing feedback modulation of periglomerular cells (M_{pg}). Without feedback modulation, the amount of overlap between output patterns increases almost linearly with the amount of overlap between input patterns ($M_{pg}=0.0$). With increasing modulation however, the overlap between output patterns is significantly lower than the overlap between input patterns.

ties due to reduced granule cell inhibition through the feedback regulation.

Fig. 9 illustrates the temporal responses of individual cells and field potentials in response to a periodic stimulus mimicking the 8 Hz sniff cycle. The membrane potentials and action potentials of four mitral cells (M1–M4) are shown along with the membrane potential of the modulator neuron (Mod) and the average membrane potentials of all granule cells (EFP). The simulation begins with no modulation, and modulation conditions are changed abruptly while the simulation is running and while a periodic stimulus is present. The activation of periglomerular cells by the Mo neuron completely suppresses mitral cell M1 and almost completely suppresses mitral cell M2, except for a brief burst at the beginning of each stimulus. Adding a decrease of granule cell inhibition leads to temporal change in spiking of activated neurons and an increasing spiking frequency. Note that the activity of mitral cell M3 is decreasing through subsequent stimulus cycles; this can be attributed to the long time constant of the modulation.

For control purposes, all output parameters (spike rates, oscillation frequencies, EEG frequencies etc.) have been checked after the modulation was added: although the dynamics of the individual neural responses change, the average population dynamics are not altered, as shown in Fig. 9B (FFT of average mitral cell and granule cell activities with and without modulation).

4. Discussion

We have demonstrated the putative role of modulation of two types of inhibition for olfactory bulb processing

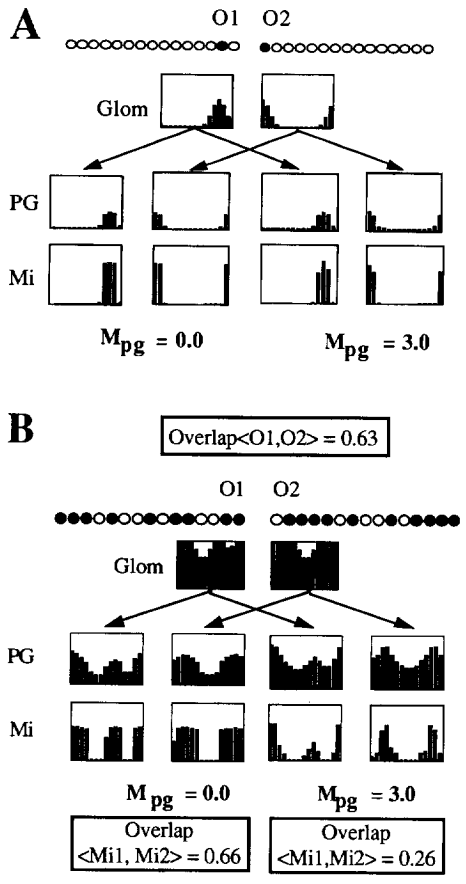

Fig. 8. Illustration of modulation effect on average periglomerular and mitral cell activities. Activity patterns in the network in response to olfactory stimuli with no ($M_{pg}=0.0$ and $M_{gm}=0.0$) modulation and with maximal ($M_{pg}=3.0$ and $M_{gm}=0.9$) modulation in response to two stimuli (O1 and O2). The first row of graphs show the total input to each of the 15 glomeruli (GLOM) (averaged over stimuli duration), the second row of graphs shows the average periglomerular cell firing probabilities (PG) and the third row the averaged mitral cell firing probabilities (Mi). (A) Two low complexity stimuli O1 and O2 (one component active) with no overlap. Due to the low number of activated mitral cells, the feedback regulation of modulation is not activated and the resulting mitral cell activity patterns is comparable with ($M_{pg}=3.0$ and $M_{gm}=0.9$) and without ($M_{pg}=0.0$ and $M_{gm}=0.0$) modulation. (B) Two high complexity (9–10 active components) input stimuli O1 and O2 with large overlap (0.63). In this example, the activity of periglomerular cells (PG) is increased by the feedback regulation of modulation ($M_{pg}=3.0$) as compared to the activity in the absence of modulation ($M_{pg}=0.0$). As a consequence, the number of active mitral cells is decreased by the feedback regulation. The overlap between the output patterns is considerably lower if feedback regulation is activated (0.26) than in absence of feedback regulation (0.66).

of olfactory stimuli: (i) feedback regulation of lateral inhibition in the glomerular layer ensures a constant average number of active mitral cells over the total input pattern space; (ii) feedback regulation of the modulation of inhibition mediated by granule cells in the deeper bulbar layers ensures constant average spiking probabilities of active mitral cells over the total input pattern space; and (iii) the combined effect of the modulation of both types of inhibition considerably decreases the over-

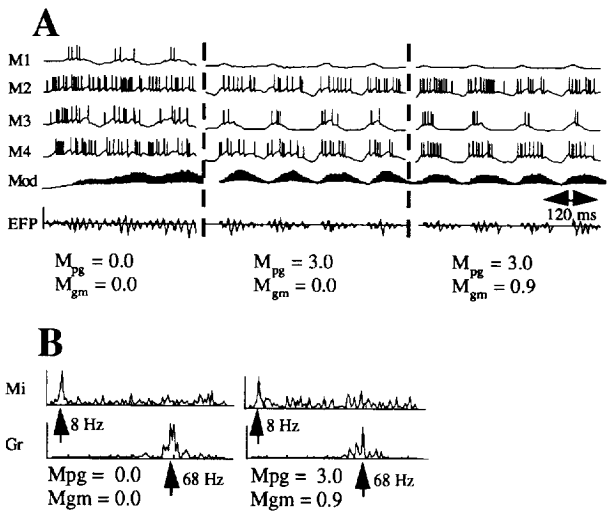

Fig. 9. Neural activity and population activity in the model for different modulation levels. (A) Membrane potentials and action potentials of four mitral cells (M1–M4) are shown along with the membrane potential of the modulator neuron (Mod) and the average membrane potentials of all granule cells (EFP). No modulation ($M_{pg}=M_{gm}=0.0$), modulation of inhibition mediated by periglomerular cells ($M_{pg}=3.0$; $M_{gm}=0.0$) and modulation of both periglomerular cells and of granule cell inhibition ($M_{pg}=3.0$; $M_{gm}=0.9$) is shown subsequently. (B) Frequency spectra (FFT) of average mitral (Mi) and granule cell (Gr) responses in the absence of modulation ($M_{pg}=0.0$; $M_{gm}=0.0$) and for maximal modulation values ($M_{pg}=3.0$; $M_{gm}=0.9$).

lap between pairs of output patterns, thus enhancing the discrimination between highly overlapping olfactory input patterns.

The implemented modulation is inspired by experimental data. ACh modulation in the glomerular layer has been shown to increase periglomerular cell activity and to decrease mitral cell responsiveness [34]. NA and ACh modulation in the granule cell layer has been shown to suppress the inhibition of mitral cells by granule cells [5,17,40]. Even though there have been some differences in the action of NA observed during in vivo experiments [30], most studies suggest a disinhibitory effect on mitral cells [18,46].

The model relies on the regulation of the activity of cholinergic and noradrenergic neurons by the activity in the olfactory bulb. Although there is no evidence for direct connections from the olfactory bulb to the HDB or the LC, relatively direct pathways exist through the medial optic area and the Medial amygdaloid area (to LC) (see [36] for review) and there appears to be at least some input via the olfactory cortex and also via the anterior cortical nucleus of the amygdala to the HDB (see [37] for review). An electrophysiological study has shown that firing rates of neurons in the horizontal limb are affected by stimulation of the olfactory bulb and of the prepiriform cortex [7].

An alternative mechanism for regulation of NA modulation is given by the now growing evidence for glutamatergic neurotransmitters directly stimulating noradrenaline release in many brain areas, including the olfactory bulb [42]. As a consequence, the feedback of the modulation would be related to local levels of mitral cell activity rather than being a function of their combined activity. In this case, the equation for the modulation in the granule cell layer (page 6) reads:

$$w_{ij}^{gm}(t)=(1.0-M_{gm})\,x_j\,(t)\,(t)\,w^{gm}(\max)$$

where $x_j(t)$ is the output of the presynaptic mitral cell, and M_{gm} is the variable modulation parameter. This results in a disinhibition of active mitral cells only, thus enhancing the effect resulting from a global modulation as we have described it.

NA modulation has been shown to be crucial for long-term storage of olfactory stimuli in various behavioral experiments [1,22,32,39] and olfactory learning in the olfactory bulb has been proposed to be localized in the interactions between mitral and granule cells [19]. The model would predict that disinhibition of mitral cells, as suggested for NA modulation [17,40] would increase mitral cell firing without decreasing mitral cell selectivity to odor stimuli. Increased neural activity in response to novel stimuli might be important for synaptic changes mediating olfactory memory. In addition, NA modulation has been shown to influence the dynamics of bulbar responses to olfactory stimuli, decreasing the habituation to familiar stimuli [9].

In the context of olfactory learning, mitral cell responsiveness to odors seems to depend strongly on the level of periglomerular inhibition Interneurons in the glomerular layer appear to use both GABA and dopamine as the inhibitory transmitter in the glomerular layer [41]. In rat pups, olfactory learning results in a decrease of the proportion of mitral cells responding by excitation and in an increase in the proportion of cells responding by inhibition to the conditioned odor [39]. A recent experiment showed, in anesthetized rat, that suppression of dopaminergic action increases the proportion of mitral cells which do not to discriminate between two odorants [47]. In sheep, monitoring dopamine (DA) release in the olfactory bulb revealed that levels of DA increased pre-partum and in the early post-partum period. Basal release is significantly higher in multiparous ewes when compared to primiparous ewes [21]. Thus, an increase in periglomerular cell activity could facilitate discrimination between different very similar and complex lamb odors and this increase in periglomerular inhibition could also partly explain spectacular changes in the proportion of mitral cells responding to lamb and non-lamb odors observed in sheep following parturition [20]. As suggested by the model, these behavioral results indicate that inhibition mediated by periglomerular cells in the glomerular layer is crucial for the separation of olfactory stimuli and that a suppression of inhibition results in higher proportions of active mitral cells as

well as in an 'over-generalization' between different stimuli.

Acknowledgement

Supported by a Human Frontier Fellowship to C. Linster and by an Office of Naval Research Young Investigator Award N00014-93-1-0595 and an NIMH award R29 MH52732-01 to M.E. Hasselmo.

Appendix: Implementation and simulation parameters

Neurons

In continuous time, the fluctuation of the membrane potential v(t) around the resting potential, due to input $e(t)$ at its postsynaptic sites, is expressed as:

$$\tau \frac{dv(t)}{dt} + v(t) = e(t)$$

In discrete time, this equation becomes:

$$v(t) = \left(1 - \frac{\Delta t}{\tau}\right) v(t - \Delta t) + \frac{\Delta t}{\tau} e(t)$$

where τ is the membrane time constant, and Δt is the sampling interval, and $e(t)$ is the total input to neuron i at time t.

The firing probability $P[x_i(t) = 1]$ that the *state* $x_i(t)$ of neuron i at time t is 1 is given by a quasi-linear function of the neuron *membrane potential* $v_i(t)$ at time t, where the lower threshold Θ_{min} determines the amount of noise, and the upper threshold Θ_{max} determines the value of the membrane potential for which the maximal firing probability is reached:

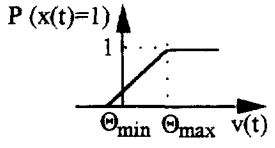

The value of the transmission delay associated with each synapse is chosen randomly around a given average value; it is meant to model all sources of delay, transduction and deformation of the transmitted signal from the cell body or dendro-dendritic terminal of neuron j to the receptor site of neuron i.

Updating of the difference equations is synchronous, with a sampling step of 2 ms.

Molecule arrays and receptor cells

Odorant components are represented in a 15-dimensional, discrete odorant space; each stimulus corresponds to a particular point in this space. R receptor cells are differentially sensitive to all M components: each receptor cell has a maximal (1) sensitivity to one molecule (center of the gaussian sensitivity curve), its sensitivity to surrounding molecules is given by a gaussian function with width 2. Each receptor cell projects onto a subset of N neighboring glomeruli with an afferent weight w_R.

Glomerular layer

Mitral cells are represented by their primary and secondary dendrites in the model.

Inside the glomerulus, mitral cell primary dendrites (M1_) receive input from receptor cells, from periglomerular cells located in the same glomerulus and from periglomerular cells located in neighboring glomeruli.

$$\mathrm{m1i}(t) = w^{\mathrm{Rm}} R_i(t) + w^{\mathrm{p}} P_i(t - d^{\mathrm{p}}) + \sum_{g \neq i}^{i+/-2} w_{ig}^{\mathrm{pm}} p_g(t - d_{ig}^{\mathrm{pm}})$$

where $m1_i(t)$ is the total input to the mitral cell connected to glomerulus i at time t, R_i is the output of the receptor cell type projecting to glomerulus i; w^{Rm} its connection strength; P_i is the output of the periglomerular cell connected to glomerulus i, w^{Rm} its connection strength and d^{p} it connection delay; P_g are the outputs of periglomerular cells connected to glomeruli g, w_{ig}^{pm} their connection strength and d_{ig}^{pm} their connection delays.

Inside their glomerulus, periglomerular cells receive input from receptor cells, from mitral cell primary dendrites located in the same glomerulus and from periglomerular cells located in neighboring glomeruli.

$$\mathrm{pg}_i(t) = w^{\mathrm{Rpg}} R_i(t) + w^{m} vm1_i(t - d^{m}) + \sum_{g \neq i}^{i+/-2} w_{ig}^{\mathrm{pp}} p_g(t - d_{ig}^{\mathrm{pp}})$$

where $\mathrm{pg}_i(t)$ is the total input to the periglomerular cell connected to glomerulus i at time t, R_i is the output of the receptor cell type projecting to glomerulus i; w^{Rpg} its connection strength; $vm1_i$ is the membrane potential of the mitral cell primary dendrite connected to glomerulus i, w^{m} its connection strength and d^{m} its connection delay; p_g are the outputs of periglomerular cells connected to glomeruli g, w_{ig}^{pp} their connection strength and d_{ig}^{pp} their connection delays.

Deeper layer

Mitral cell secondary dendrites represent the integration site for all mitral cell input; they receive input from mitral cell primary dendrites and from granule

cells:

$$m_i(t) = \alpha v\mathrm{m1}_i(t-\Delta t) + \sum_{g}^{G} w_{ig}^{\mathrm{gm}} G_g(t-d_{ig}^{\mathrm{gm}})$$

where $m_i(t)$ is the total input to a mitral cell connected to glomerulus i; $v\mathrm{m1}_i$ is the membrane potential resulting from synaptic interactions in the glomerulus, α a decay constant, Δt the sampling step; G_g is the output of the granule cell population close to glomerulus g (to each glomerulus is associated one population of granule cells represented by G_g), w_{ig}^{gm} its weight and d_{ig}^{gm} its connection delay. The effect of granule cells onto mitral cells takes place over long distances, but does not decrease as a function of the distance between glomerulus i and glomerulus j; the effect of the distance is taken into account only in the connection strength and connection delays describing the excitatory effect of mitral cells onto granule cells.

Granule cells receive input from mitral cells as well as from close granule cells:

$$gi(t) = \sum_{g}^{i=g+/-5} w_{ig}^{\mathrm{mg}} M_g(t-d_{ig}^{\mathrm{mg}}) + \sum_{g\neq i}^{i=g+/-3} W_{ig}^{\mathrm{gg}} G_g(t-d_{ig}^{\mathrm{gg}})$$

where g_i is the total input to granule cell close to glomerulus i, M_g is the output of a mitral cell connected to glomerulus g, w_{ig}^{mg} its connection strength (which decreases as the distance between i and g increases), d_{ig}^{mg} its connection delay (which increases as the distance between i and g increases); G_g is the output of a granule cell close to glomerulus g, w_{ig}^{gg} its connection strength and d_{ig}^{gg} its connection delay.

Parameter values

Mi1: $\tau = 10$ ms; $\theta_{\min} = -0.1$; $\theta_{\max} = 1.0$.

PG: $\tau = 2.5$ ms; $\theta_{\min} = -0.1$; $\theta_{\max} = 6.0$.

Mi2: $\tau = 10$ ms; $\theta_{\min} = -0.1$; $\theta_{\max} = 1.0$

GR: $\tau = 4$ ms; $\theta_{\min} = -0.1$; $\theta_{\max} = 0.5$

Mo$\tau = 50$ ms; $\theta_{\min} = 0.5$; $\theta_{\max} = 1.0$

Afferent connections:

$w^{\mathrm{Rm}} = 4.0(+/-10\%)$

$w^{\mathrm{Rpg}} = 1.0(+/-10\%)$

Intra-glomerular connections:

$w^{\mathrm{p}} = -0.5(+/-10\%)$; $d^{\mathrm{p}} = 2ms$

$w^{\mathrm{m}} = 1.0(+/-10\%)$; $d^{\mathrm{m}} = 2ms$

inter-glomerular connections:

$w_{ig}^{\mathrm{pm}} = -2.0(+/-10\%)$; $d_{ig}^{\mathrm{pm}} = 2--6$ms,

$w_{ig}^{\mathrm{pp}} = -0.2(+/-10\%)$; $d_{ig}^{\mathrm{pm}} = 2--6$ms,

each periglomerular cell connects to four surrounding glomeruli.

Deeper layer:

$w_{ig}^{\mathrm{gm}} = -0.2(+/-10\%)$, $d_{ig}^{\mathrm{gm}} = 12ms(+/-10\%)$;

$w_{ig}^{\mathrm{mg}}(\max) = 0.5$ between neighboring cells, w_{ig}^{gm} decreases linearly towards 0 (maximal distance between two connected cells is 5 columns), $d_{ig}^{\mathrm{gm}}(\min) = 2$ ms, increases linearly towards 10 ms; $w_{ig}^{\mathrm{gg}}(\max) = -0.3$, decreases linearly towards -0.1 (maximal distance between two connected cells is 3 columns), $d_{ig}^{\mathrm{gg}} = 6$ ms.

References

[1] Brennan, P., Kaba, H., Keverne, E.B., Olfactory recognition: a simple memory system, *Science*, 250 (1990) 1223–1226.

[2] Buonoviso, N. and Chaput, M., Response similarity to odors in olfactory bulb output cells presumed to be connected to the same glomerulus: electrophysiological study using simultaneous single-unit recordings, *J. Neurophysiol.*, 63 (1990) 447–454.

[3] Chaput, M.A. and Holley, A., Single unit responses of olfactory bulb neurons to odor presentation in awake rabbits, *J. Physiol. (Paris)*, 76 (1980) 551–558.

[4] Edelmann, J.A. and Freeman, W.J., Simulation and analysis of a model of Mitral/granule cell population interactions in the mammalian olfactory bulb, *Proceedings IJCNN-90-Wash-DC*, Caudill (Ed.),Vol. 1, 1990, pp. 62–65.

[5] Elaagouby, A., Ravel, N. and Gervais, R., Cholinergic modulation of excitability in the rat olfactory bulb: effect of local application of cholinergic agents on evoked field potentials, *Neuroscience*, 45(3) (1992) 653–662.

[6] Erdi, P., Gröbler T., Barna, G. and Kaski, K., Dynamics of the olfactory bulb: bifurcations, learning and memory, *Biol. Cybern.*, (69) (1993) 57–66.

[7] Ferreyra-Moyano, H. and Molina, J.C., Olfactory connections of substantia innominata and nucleus of the horizontal limb of the diagonal band in the rat: an electrophysiological study, *Neurosci. Lett.*, 34(3) (1982) 241–246.

[8] Freeman, W. and Schneider, W.S., Changes in spatial patterns of rabbit olfactory EEG with conditioning to odors, *Psychophysiology*, 19 (1982) 44–56.

[9] Gray, C.M., Freeman, W.J. and Skinner, J.E., Chemical dependencies of learning in the rabbit olfactory bulb: acquisition of the transient spatial pattern change depends on norepinephrine, *Behav. Neurosci.*, 100(4) (1986) 585–596.

[10] Haberly, L.B. and Bower, J.M., Olfactory cortex: model circuit for study of associative memory, *Trends Neurosci.*, 12 (1989) 258–264.

[11] Halasz, H. and Shepherd, G.M., Neurochemistry of the vertebrate olfactory bulb, *Neuroscience*, 19 (1983) 579–619.

[12] Hasselmo, M.E., Neuromodulation and cortical function: Modeling the physiological basis of behavior, *Behav. Brain. Res.*, 67 (1995) 1–27.

[13] Hasselmo, M.E., Anderson, B.P. and Bower, J.M., Cholinergic modulation of cortical associative memory function, *J. Neurophysiol.*, 67 (1992) 1239–1246.

[14] Hasselmo, M.E. and Bower, J.M., Acetycholine and Memory, *Trends Neurosci.*, 16(6) (1993) 218–222.

[15] Hasselmo, M.E. and Schnell, E., Laminar selectivity of the cholinergic suppression of synaptic transmission in rat hippocampal region CA1: computational modeling and brain slice physiology, *J. Neurosci.*, 14(6) (1994) 3898–3914.

[16] Holley, A., Neural coding of olfactory information. In: T.V.

Getchell et al. (Eds.), *Smell and Taste in Health and Disease*, New York, Raven Press, 1991, pp. 329–343.

[17] Jahr, C.E. and Nicoll, R.A., Noradrenergic modulation of dendrodendritic inhibition in the olfactory bulb, *Nature*, 297 (1982) 227–229.

[18] Jiang, M., Griff, E.R., Zimmer, L.A., Ennis, M. and Shipley, M.T., Locus coerulus increases perithreshold sensory-evoked excitation of mitral cells, *Abstract, 15th Ann. Meeting of AChems, Sarasota*, 1993.

[19] Kaba, H., Hayashi, Y., Higuchi, T., Nakanishi, S., Induction of an olfactory memory by the activation of a metabotropic glutamate receptor, *Science*, 26 (1994) 262–264.

[20] Kendrick, K.M., Levy, F. and Keverne, E.B., Changes in the sensory processing of olfactory signals induced by birth in sheep, *Science*, 256 (1992) 833–836.

[21] Keverne, E.B., Levy, F., Guevara-Guzman, M. and Kendrick, K.M., Influence of birth and maternal experience on olfactory bulb neurotransmitter release, *Neuroscience*, 56 (1993) 557–565.

[22] Levy, F., Gervais, R., Kindermann, U., Orgeur, P. and Piketty, V., Importance of -noradrenergic receptors in the olfactory bulb of sheep for recognition of lambs, *Behav. Neurosci.*, 104 (1990) 464–469.

[23] Li, Z. and Hopfield, J.J., Modeling the olfactory bulb and its neural oscillatory processings, *Biol. Cybern.*, 61 (1989) 379–392.

[24] Li, Z., A model of olfactory adaptation and sensitivity enhancement in the olfactory bulb, *Biol. Cybern.*, 62 (1990) 349–361.

[25] Linster, C. and Gervais, R., Investigation of the role of interneurons and their modulation by centrifugal fibers in a neural model of the olfactory bulb, *J. Comput. Neurosci.*, 3(3) (1996) 225–246.

[26] Linster, C., Hasselmo, M.H. and Gervais, R., *Soc. of Neuroscience Abstr.*, 1995.

[27] Linster, C., Masson, C., Kerszberg, M., Personnaz, L. and Dreyfus, G., Computational Diversity in a formal model of the insect macroglomerulus, *Neural. Comput.*, 5 (1993) 239–252.

[28] Macrides, F., Davis, B.J., Youngs, W.M., Nadi, N.S. and Margolis, F.L. (1981) Cholinergic and catelolaminergic afferents to the olfactory bulb in the hamster: a neuroanatomical, biochemical and histochemical investigation, *J. Comp. Neurol.*, 203 (1981) 497–516.

[29] Meredith, M., Neural circuit computation: Complex patterns in the olfactory bulb, *Brain Res. Bull.*, 29 (1992) 111–117.

[30] Mouly, A.-M., Elaagouby, A. and Ravel, N., A study of the effects of noradrenaline in the rat olfactory bulb using evoked field potential response, *Brain Res.*, 681 (1995) 47–57.

[31] Pager, J., Unit responses changing with behavioral outcome in the olfactory bulb of unrestrained rats, *Brain Res.*, 289 (1983) 87–98.

[32] Pissonnier, T., Fabre-Nys, C., Poindro, P. and Keverne, E.B., The importance of olfactory bulb noradrenaline for maternal recognition in sheep, *Physiol. Behav.*, 35 (1985) 361–364.

[33] Rall, W. and Shepherd, G.M., Theoretical reconstruction of field potentials and dendrodendritic synapse interaction in olfactory bulb, *J. Neurophysiol.*, 31 (1968) 884–915.

[34] Ravel, N., Akaoka, H., Gervais, R. and Chouvet, G., The effect of acetycholine on rat bulbar unit activity, *Brain Res. Bull.*, 24 (1990) 1–5.

[35] Ravel, N., Elaagouby, A. and Gervais, R., Scopolamine injection into the olfactory bulb impairs short-term olfactory memory, *Behav. Neurosci.*, 108 (1994) 317–324.

[36] Rizni, T.A., Ennis, M., Aston-Jones, G., Jiang, M., Liu, W., Behbehani, M.M. and Shipley, M.T., Preoptic projections to barrinton's nucleus and the pericoerular region architecture and terminal organization, *J. Comp. Neurol.*, 347 (1994) 1–24.

[37] Russchen, F.T., Amral, D.G. and Price, J.L., The afferent connections of the substantia innominata in the monkey, *Macaca fascicularis*, *J. Comp. Neurol.* 242 (1985) 1–27.

[38] Scott, J.W., Wellis, D.P., Riggott, M.J. and Buonoviso, N., Functional organization of the main olfactory bulb, *Microsc. Res. Tech.* 24 (1993) 142–156.

[39] Sullivan, R.M., Wilson, D.A. and Leon, M., Norepinephrine and learning-induced plasticity in infant rat olfactory system, *J. Neurosci.*, 9 (1989) 3998–4006.

[40] Trombley, P.Q. and Shepherd, G.M., Noradrenergic inhibition of synaptic transmission between mitral and granule cells in mammalian olfactory bulb cultures, *J. Neurosci.*, 12(10) (1992) 3984–3991.

[41] Trombley, P.Q. and Shepherd, G.M., Synaptic transmission and modulation in the olfactory bulb, *Curr. Opin. Neurobiol.*, 3 (1993) 540–547.

[42] Wang, J.K., Andrews, H. and Thurkrai, V., Presynaptic glutamate receptors regulate noradrenaline release from isolated nerve terminals, *J. Neurochem.*, (58) (1992) 204–211.

[43] Wellis, D.P. and Kauer, J.S., GABAergic and glutamaergic synaptic input to identified granule cells in salamander olfactory bulb, *J. Neurophysiol.*, 475(3) (1994) 419–430.

[44] Wellis, D.P. and Scott, W.J., Intracellular responses of identified rat olfactory bulb interneurones to electrical and odor stimulus, *J. Neurophysiol.*, 64 (1990) 932–947.

[45] White, J., Hamilton, K.A., Neff, S.R. and Kauer, J.S., Emergent properties of odor information coding in a representational model of the salamander olfactory bulb, *J. Neurosci.*, 5 (1992) 1772–1780.

[46] Wilson, D.A. and Leon, M., Noradrenergic modulation of olfactory bulb excitability in the postnatal rat, *Dev. Brain Res.*, 42 (1988) 69–75.

[47] Wilson, D.A. and Sullivan, R.M., The D2 antagonist spiperone mimics the effects of olfactory deprivation on mitral/tufted cell odor response patterns, *J. Neurosci.*, 15(8) (1995) 5574–5581.